

## FEM Analysis of Eddy Currents in Coated PM of Surface-Mounted-PM SM

Yoshida, Kinjiro

Department of Electrical and Electronic Systems Engineering, Faculty of Information Science and Electrical Engineering, Kyushu University

Nakayama, Seiji

Department of Electrical and Electronic Systems Engineering, Graduate School of Information Science and Electrical Engineering, Kyushu University : Graduate Student

<https://doi.org/10.15017/1515735>

---

出版情報 : 九州大学大学院システム情報科学紀要. 6 (2), pp.191-196, 2001-09-26. 九州大学大学院システム情報科学研究所

バージョン :

権利関係 :



## FEM Analysis of Eddy Currents in Coated PM of Surface-Mounted-PM SM

Kinjiro YOSHIDA\* and Seiji NAKAYAMA\*\*

(Received June 15, 2001)

**Abstract:** Recently the rare-earth magnet NdFeB is applied to a magnet motor of electric vehicles. The rise of temperature due to eddy current loss in the PM (Permanent Magnet) leads to serious deterioration of the PM, especially in high speed operation. In general NdFeB is coated with Ni(Nickel) or Al(Aluminum) in order to prevent from corrosion and destruction. PM coating is very thin, but conductivity of coating material is much larger than that of PM, and Ni is the magnetic material. Consequently, PM coating has an influence on the eddy currents in PM. This paper presents the finite element analysis of eddy currents in coated PM of surface-mounted-PM SM (Synchronous Motor), and makes clear an influence of Al- and Ni-coating.

**Keywords:** PM-SM, Finite element method, Analysis of eddy current, PM coating

### 1. Introduction

For electric vehicles, the rare-earth magnet, such as SmCo, NdFeB etc, are applied to a magnet rotor of the motor. The conductivity of their magnets is higher compared with that of ferrite magnet. In the high speed operation, the loss due to eddy currents produced in the PM cannot be neglected. To reduce the eddy current loss in the PM, the authors presented the eddy currents analysis in the PM of surfaced-mounted-PM SM<sup>1)</sup>, and proposed the schemes, i.e. the segmented PM<sup>2,3)</sup> and the insulated PM<sup>4)</sup>. Generally NdFeB is coated with Ni or Al. An influence of these coating has not been made clear.

This paper describes FEM analysis and an influence of Al- and Ni-coating, FEM (Finite element method) mesh of coated-PM and magnetic saturation of Ni-coating on eddy currents in PM.

### 2. PM SM model

Figure 1 shows an analysis model of the four-pole surfaced-mounted-PM SM. It has a rating of 1.94kW and the rotor consists of NdFeB magnets. The diameter of rotor is 78mm, the gap length is 1mm, the thickness of PM is 3mm and the stack length of rotor is 76mm.

Table 1 shows specification for PM SM.

Figure 2 shows the 6-segmented magnet. In the 6-segmented magnet, the direction of magnetization changes gradually from one segment to

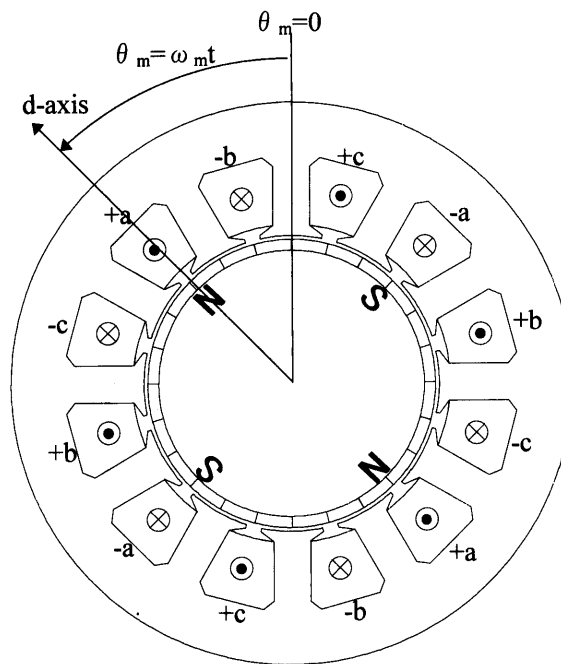


Fig.1 Surface-Mounted-PM SM.

another so that the airgap flux density distribution would be sinusoidal approximately. An insulator with thickness of 25  $\mu\text{m}$  is inserted into gap between each PM segment.

Figure 3 shows the form of one segment of PM. Figure 3 (a) is non-coated PM segment with insulator in both sides. Figure 3 (b) is PM segment coated all around with very thin Al or Ni material. The thickness of PM coating is 13.4  $\mu\text{m}$ . A coated PM segment also has the insulator in both sides. The coating part is expanded and displayed in order to make it legible.

\* Department of Electrical and Electronic Systems Engineering

\*\* Department of Electrical and Electronic Systems Engineering, Graduate Student

Table 1 Specification for PM SM.

Ratings		Stator		Rotor	
Power	1.94kW	Number of coils per phase	2	Diameter	φ78mm
Poles	4	Number of coils per turns	110	Material of PM	NdFeB
Speed	1800rpm	Slots	12	Thickness of PM	3mm
Voltage	277.8V	Series turns per phase	220	Thickness of insulation between PM's	0.025mm
Current	4.33A	Material of core	S18	Material of core	S45C
Frequency	60Hz	Inner diameter	φ80mm	Diameter of core	72mm
Stack length	76mm	Outer diameter	φ150mm		

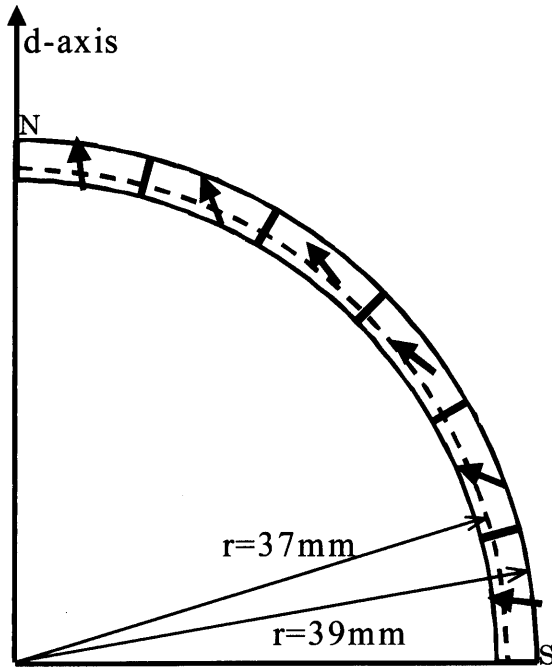


Fig.2 PM magnetization.

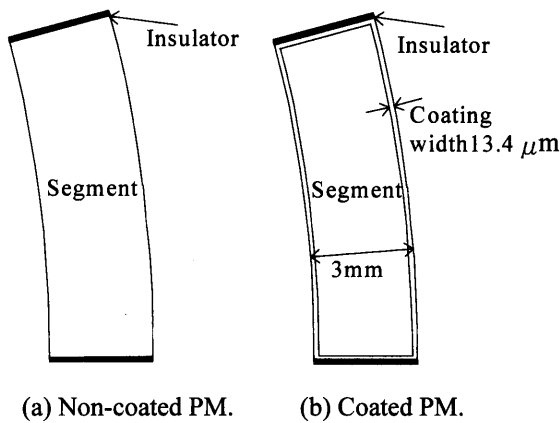


Fig.3 One segment of PM.

### 3. Analysis method

#### 3.1 Finite element method

The two-dimensional magnetic field is analyzed by the following equation:

$$\frac{\partial}{\partial x} \left( \nu \frac{\partial A}{\partial x} \right) + \frac{\partial}{\partial y} \left( \nu \frac{\partial A}{\partial y} \right) = - J_0 - J_e - J_m \quad (1)$$

$$J_e = - \sigma \frac{\partial A}{\partial t} - \sigma \frac{\partial \phi}{\partial z} \quad (2)$$

$$J_m = \nu_0 \left( \frac{\partial M_y}{\partial x} - \frac{\partial M_x}{\partial y} \right) \quad (3)$$

where  $A$  is the magnetic vector potential,  $J_0$ ,  $J_e$  and  $J_m$  are the source current, the equivalent magnetizing current density, and the eddy current density, respectively,  $M_x$  and  $M_y$  are the component of x-y axis magnetize,  $\sigma$  is the conductivity,  $\phi$  is the scalar electric potential, and  $\nu$  is the reluctivity. FEM matrix equation is derived as

$$\begin{bmatrix} \frac{\partial G_1^t}{\partial A_1} & \dots & \frac{\partial G_1^t}{\partial A_n} \\ \vdots & \ddots & \vdots \\ \frac{\partial G_i^t}{\partial A_j} & \dots & \dots \\ \vdots & \dots & \vdots \\ \frac{\partial G_n^t}{\partial A_1} & \dots & \frac{\partial G_n^t}{\partial A_n} \end{bmatrix} \begin{bmatrix} \delta A_1^t \\ \vdots \\ \delta A_i^t \\ \vdots \\ \delta A_n^t \end{bmatrix} = \begin{bmatrix} -G_1^t \\ \vdots \\ -G_i^t \\ \vdots \\ -G_n^t \end{bmatrix} \quad (4)$$

in above equation,

$$G_i^{(e)t} = \nu^{(e)t} U_{ie} - \frac{\Delta^{(e)}}{3} J_0^{(e)t} - J_{ei}^{(e)t} - J_{mi}^{(e)t} \quad (5)$$

$$\frac{\partial G_i^t}{\partial A_j^t} = \sum_{e=1}^{ne} \left\{ \frac{2}{\Delta^{(e)}} \frac{\partial \nu^{(e)t}}{\partial (B^{(e)t)^2} } U_{ie} U_{je} + \nu^{(e)t} S_{ij}^{(e)} - \frac{\partial J_{ei}^{(e)t}}{\partial A_j^t} \frac{\partial J_{mi}^{(e)t}}{\partial A_j^t} \right\} \quad (6)$$

where

$$J_{ei}^{(e)t} = -\frac{\sigma\Delta^{(e)}}{12} \sum_{j=1}^3 (1 + \delta_{ij}) \frac{A_{je}^t - A_{je}^{t-\Delta t}}{\Delta t} + \frac{\sigma}{S^{(l)}} \frac{\Delta^{(e)}}{3} \sum_{e\phi=1}^{N^{(l)}} \left\{ \frac{\Delta^{(e\phi)}}{3} \sum_{k=1}^3 \frac{\partial A_{k\phi}^t}{\partial t} \right\} \quad (7)$$

$$J_{mi}^{(e)t} = \frac{\nu_0}{2} (M_x^t d_{ie} - M_y^t c_{ie}) \quad (8)$$

$$U_{ie} = \sum_{j=1}^3 S_{ij}^{(e)} A_{je}^t \quad (9)$$

$$S_{ij}^{(e)} = \frac{1}{4\Delta^{(e)}} (c_{ie} c_{je} + d_{ie} d_{je}) \quad (10)$$

and

$$\frac{\partial J_{ei}^{(e)t}}{\partial A_j^t} = -\delta \frac{\Delta^{(e)}}{12} (1 + \delta_{ij}) \frac{1}{\Delta t} + \frac{\sigma}{S^{(l)}} \frac{\Delta^{(e)}}{3} \sum_{e\phi=1}^{N^{(l)}} \left\{ \frac{\Delta^{(e\phi)}}{3} \sum_{k=1}^3 \delta_{j,k\phi} \right\} \quad (11)$$

$$\frac{\partial J_{mi}^{(e)t}}{\partial A_j^t} = \frac{\nu_0}{4\Delta^{(e)}} \frac{\partial M_d^t}{\partial B_d^t} (d_{ie} \cos \theta^{(e)} - c_{ie} \sin \theta^{(e)}) \times (d_{je} \cos \theta^{(e)} - c_{je} \sin \theta^{(e)}) \quad (12)$$

where  $\Delta^{(e)}$  is the area of triangular element,  $A_{je}$  is the magnetic vector potential of node number  $je$ ,  $M_d$  and  $\theta^{(e)}$  are the magnetize  $M$  of  $e$ , angular from  $x$ -axis, respectively,  $B_d$  is the  $\theta$  direction component of magnetic flux density,  $S^{(e)}$  is the region of element  $e$ ,  $\nu^{(e)}$  is the reluctivity of element  $e$ ,  $S^{(l)}$  and  $N^{(l)}$  are the cross sectional area and number of element that of element  $e$  belongs to conductor  $l$ ,  $e\phi$  is the element belongs to conductor  $l$ ,  $k\phi$  is the node belongs to element  $e\phi$ ,  $\delta_{ij}$  is the klonecker's delta, when  $i=j$ ,  $\delta_{ij}=1$ .

$\partial A / \partial t$  is given by

$$\frac{\partial A^t}{\partial t} = \frac{A^t - A^{t-\Delta t}}{\Delta t} \quad (13)$$

$$c_{ie} = y_{je} - y_{ke}, d_{ie} = x_{ke} - x_{je} \quad (14)$$

where  $i_e$ ,  $j_e$  and  $k_e$  are the circulating numbers,  $x_{je}$  and  $y_{je}$  are  $x$  and  $y$  coordinates of node  $j$ .

Source current is obtained from:

$$J_0^{(e)t} = \frac{\beta^{(e)}}{\Delta t} (a_a^{(e)} W_a^{(e)} i_a^t + a_b^{(e)} W_b^{(e)} i_b^t + a_c^{(e)} W_c^{(e)} i_c^t) \quad (15)$$

$W_a^{(e)}$ ,  $W_b^{(e)}$ , and  $W_c^{(e)}$  are number of windings per element  $e$ .  $\beta^{(e)}$ ,  $a_a^{(e)}$ ,  $a_b^{(e)}$  and  $a_c^{(e)}$  are defined by:

$\beta^{(e)} = \pm 1$  (+: the conductor including element  $e$  is first half. -: the conductor including element  $e$  is return half.)

$\alpha_i^{(e)}$ : when the conductor including element  $e$  is contained by  $i$  phase windings,  $\alpha_i^{(e)} = 1$ . else  $\alpha_i^{(e)} = 0$ .

Solved equation (4), correcting value  $\delta A_i^t$  is obtained. Approximate value is given by

$$A_i^{t(m+1)} = A_i^{t(m)} + \delta A_i^{t(m)} \quad (16)$$

Eddy current density of each node is obtained from:

$$J_{e,i}^t = \frac{J_{ei}^t}{\Delta_{\phi,i}^{(l)}} \quad (17)$$

$\Delta_{\phi,i}^{(l)}$  is the area of node  $i$  in conductor  $l$ .

$$\Delta_{\phi,i}^{(l)} = \sum_{e\phi=1}^{N^{(l)}} \sum_{k=1}^3 \frac{\Delta^{(e\phi)}}{3} \delta_{i,k\phi} \quad (18)$$

Eddy current loss of each node is given by

$$P_{e,i}^t = \frac{1}{\sigma} J_{e,i}^t{}^2 \cdot \Delta_{\phi,i}^{(l)} \cdot L_s \quad (19)$$

where  $L_s$  is the effective length.

### 3.2 Analysis process

Analysis process is shown as follows:

- Give the phase current effective value  $I$ , the mechanical load angle  $\delta_m$ , and the rotor angle  $\theta_m$ .
- Give the three phase current.

$$i_a^t = \sqrt{2} I \cos(\omega t + 2\delta_m)$$

$$i_b^t = \sqrt{2} I \cos\left(\omega t + 2\delta_m - \frac{2}{3}\pi\right) \quad (20)$$

$$i_c^t = \sqrt{2} I \cos\left(\omega t + 2\delta_m - \frac{4}{3}\pi\right)$$

- Solve the non-linear problem by the Newton Rapson method.

- Judge the convergence of vector potential.

$\delta_m$  is the mechanical load angle. Where  $\delta_m = 90^\circ$ .

Assumption temperature of PM is  $140^\circ\text{C}$ , magnetization  $M$  is given by

$$M = 0.0226B + 0.8796 \quad (21)$$

The finite element analysis is carried out each 1.5 degrees of rotor position. Considering periodicity of distribution of eddy current, analysis of eddy current finish at  $\theta_m = 30^\circ$ .

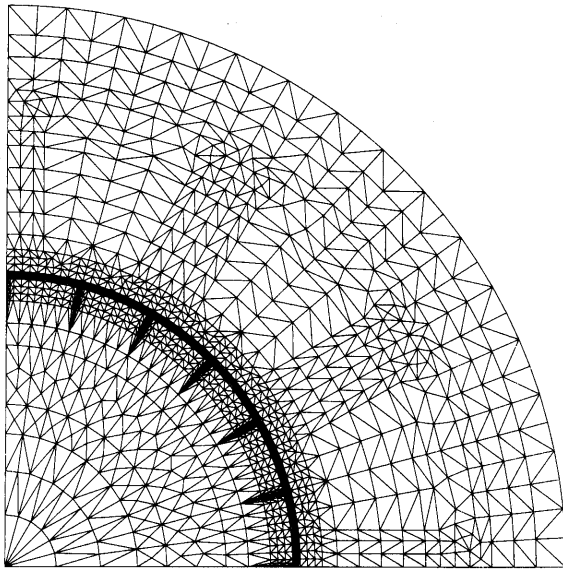


Fig.4 Finite element subdivision.

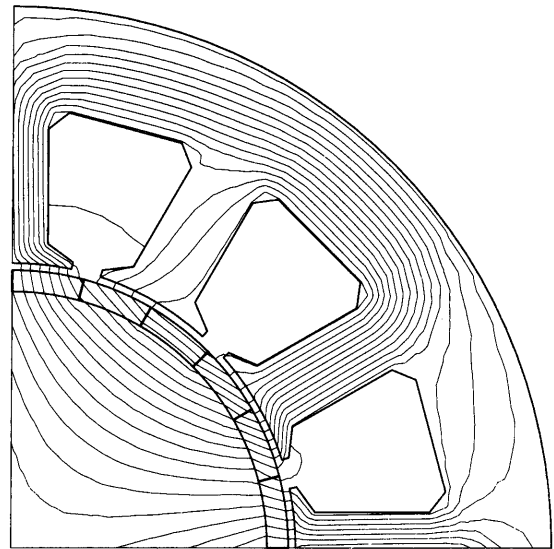


Fig.6 Flux distribution with Al-coating  
( $\theta_m = 90^\circ, 1800\text{rpm}$ ).

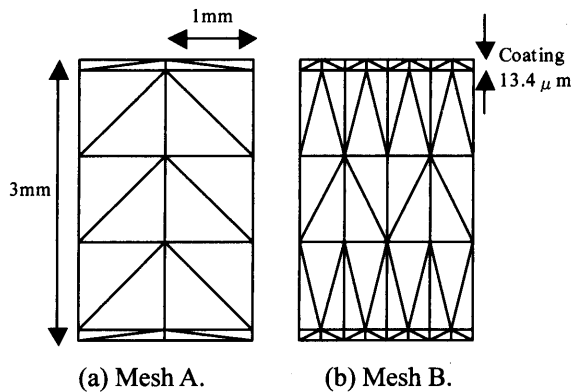


Fig.5 Finite element subdivision in PM.

The instantaneous distributions of eddy currents of coated PM were calculated numerically at the speed of 1800rpm.

The conductivity  $\sigma$  and permeability  $\mu$  of PM are  $0.69 \times 10^6$  S/m and  $\mu_0$ , respectively. PM is coated with Ni or Al. The conductivity  $\sigma$  and permeability  $\mu$  of Al are  $2.82 \times 10^7$  S/m and  $\mu_0$ . Those of Ni are  $1.0 \times 10^7$  S/m and  $500 \mu_0$  in linear analysis. Magnetic saturation is considered in non-linear analysis.

Figure 4 shows finite element subdivision.

Figure 5 shows finite element subdivision of one part of PM. Figure 5 (a) is mesh A and Figure 5 (b) is mesh B for more detailed analysis.

Figure 6 shows the flux distribution with Al-coating.

## 4. Analytical result

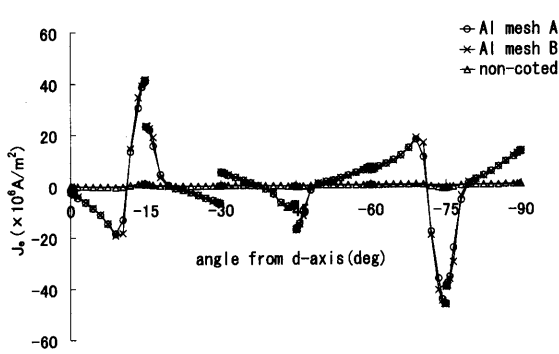
### 4.1 Al-coating

Figure 7 shows the instantaneous distributions of eddy currents in using Al-coating. At the surface of PM (radius  $r=39\text{mm}$ ), the instantaneous values of eddy-current for Al-coating are larger than those of non-coated for difference of conductivity. At the inside of PM (radius  $r=37\text{mm}$ ), the instantaneous values of eddy-current for Al-coating are approximately equal to those of non-coated. The difference of two kind of mesh has little influence on eddy currents.

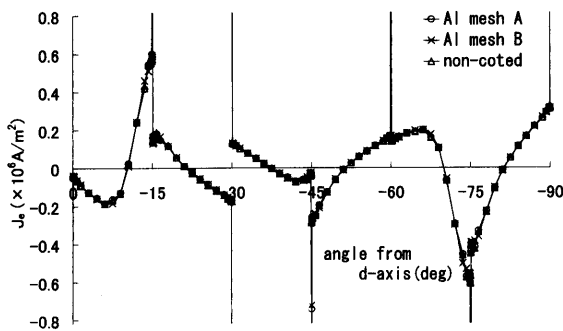
### 4.2 Ni-coating

Figure 8 and 9 show the instantaneous distributions of eddy currents in using mesh A and mesh B. In all graphs, the instantaneous values of eddy-current with mesh A are almost equal to those of mesh B.

Figure 10 shows the instantaneous distributions of eddy current with Ni coating by linear and non-linear analysis. In linear analysis, at the inside of PM (radius  $r=37\text{mm}$ ), the instantaneous values of eddy-current for Ni-coating are smaller than those of non-coated. But in non-linear analysis the permeability is close to  $\mu_0$  due to the magnetic saturation. As a result the instantaneous values of eddy-current are approximately equal to those of non-coated.

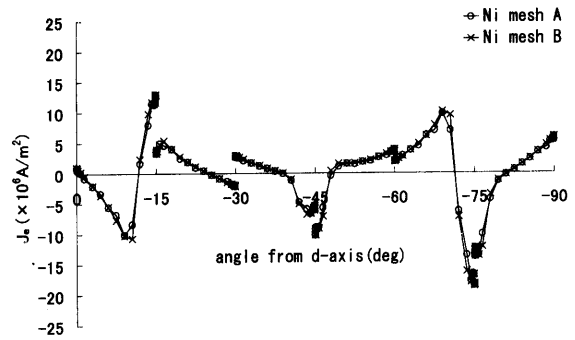


(a) Coating part(r=39mm).

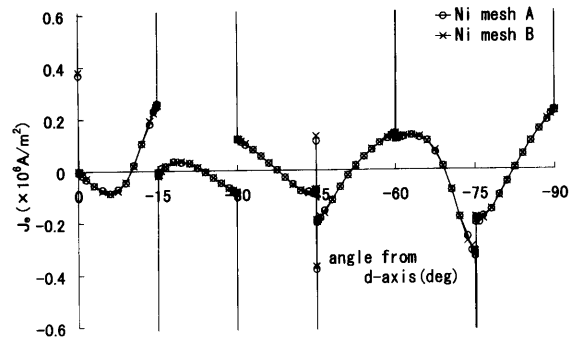


(b) Inside PM(r=37mm).

Fig.7 Distribution of eddy currents with Al-coating.

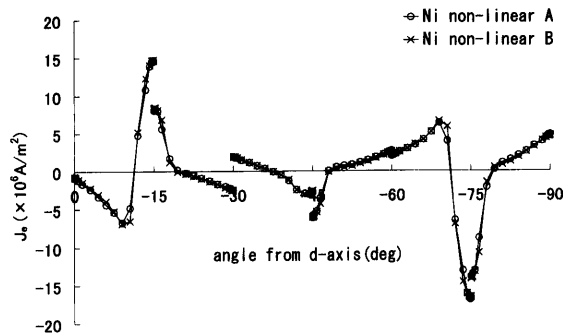


(a) Coating part(r=39mm).

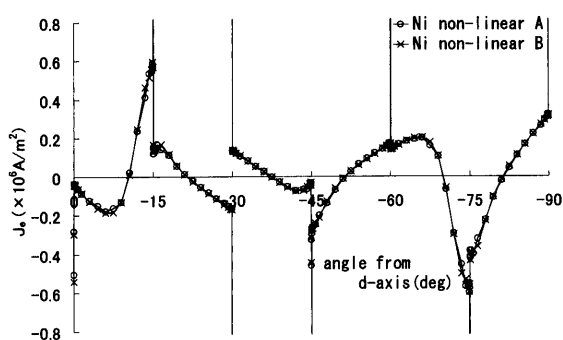


(b) Inside PM(r=37mm).

Fig.8 Distribution of eddy currents with Ni-coating by linear analysis.

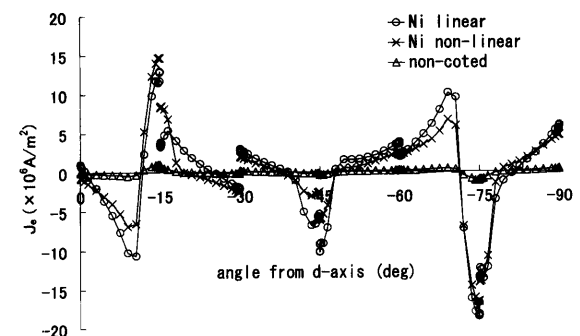


(a) Coating part (r=39mm).

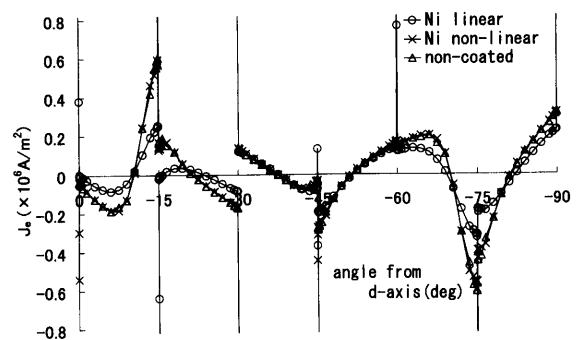


(b) Inside PM(r=37mm).

Fig.9 Distribution of eddy currents with Ni-coating by non-linear analysis.



(a) Coating part(r=39mm).



(b) Inside PM(r=37mm).

Fig.10 Distribution of eddy currents.

Table 2 Eddy current loss.

Coating material	Permeability	Mesh	Power $P$ (kW)	Eddy current loss $P_e$ (W)	$P_e/P$ (%)
Non coated	-	A	1.66	3.02	0.18
Nickel	$500 \mu_0$	A	1.34	1.79	0.13
		B	1.35	1.83	0.14
	Non-linear	A	1.66	3.66	0.22
		B	1.66	3.94	0.24
Aluminum	$\mu_0$	A	1.66	5.18	0.31
		B	1.66	5.41	0.33

### 4.3 Eddy current loss

Table 2 shows the eddy current loss in the PM and coating part for each simulation pattern. In Al-coating part extra eddy current loss is produced and the total eddy current loss  $P_e$  increases by 79% as compared with that of non-coated PM. In Ni-coating, the total eddy current loss also increases by 30% due to extra eddy current loss in coating part.

### 5. Conclusion

By FEM, the eddy currents analysis of coated PM of surfaced-mounted-PM SM has been presented. In Ni-coating analysis magnetic saturation should be considered. Extra eddy current loss due to Ni- and Al-coating have strong influence on the total eddy current loss in coated PM. From the viewpoint of total eddy current loss in Ni- and Al-coated PM, Ni-coating is better than Al-coating.

### References

- 1) K. Yoshida, Y. Hita and K. Kesamaru: "Eddy Current Loss Analysis in PM of Surface-Mounted-PM SM For Electric Vehicles", COMPUMAG Sapporo pp.324-325, October, 1999.
- 2) K. Yoshida, K. Kesamaru and Y. Hita: "Analysis of Eddy Currents in PM of Surface-Mounted PM SM", Research Reports on ISEE of Kyushu University, Vol. 2, No. 2, September 1997.
- 3) K. Yoshida, K. Kesamaru and Y. Hita: "Analysis of Eddy Currents in PM of Surface-Mounted-PM SM", Trans. IEE Japan, Vol. D-107, No. 10, October 1997.
- 4) K. Yoshida, K. Kesamaru and Y. Hita: "Eddy Currents Analysis of Surface-Mounted-PM SM by Finite Element Method", Proc. of ICEM, Istanbul, September 1998.
- 5) T. Nakata, N. Takahashi and Y. Kawase: "Consideration of Physical Meaning by the Electric Field ( $\text{grad } \phi$ ) on Eddy Currents Analysis", Papers of Technical Meeting on Information Processing, IP-89-49, IEE Japan, pp.21-30, 1980.